

# Kinetics and Mechanism of the Thermal Chlorination of Chloroform in the Gas Phase

G. HUYBRECHTS, Y. HUBIN,\* B. VAN MELE

Laboratorium voor Fysische Scheikunde en Polymeren, Vrije Universiteit Brussel, 1050 Brussels, Belgium

Received 9 October 1998; accepted 6 March 2000

**ABSTRACT:** The gas-phase thermal chlorination of  $\text{CHCl}_3$  has been studied up to high conversions by photometry and gas chromatography in a conditioned static quartz reaction vessel between 573 and 635 K. The initial pressures of both  $\text{CHCl}_3$  and  $\text{Cl}_2$  ranged from about 10–100 Torr, and the initial total pressure was varied between about 30–190 Torr. The reaction is rather complex because the produced  $\text{CCl}_4$  is not stable. The rate of consumption of  $\text{Cl}_2$  therefore increases in the course of time. This acceleration is explained quantitatively in terms of a radical mechanism and its kinetic and thermodynamic parameters. This reaction model is based on a known model for the pyrolysis of  $\text{CCl}_4$  to which only one reaction couple involving  $\text{CHCl}_3$  has been added. Analyses of the rates of the homogeneous elementary steps show that the primary source of Cl atoms is the second-order dissociation of  $\text{Cl}_2$ , which is rapidly superseded by a secondary source, the first-order dissociation of the  $\text{CCl}_4$  primary product.

© 2000 John Wiley & Sons, Inc. *Int J Chem Kinet* 32: 466–472, 2000

## INTRODUCTION

Despite conditioning of the reactors, the gas-phase chain thermal chlorinations and the chlorine-catalyzed pyrolyses of hydrocarbons or partially chlorinated hydrocarbons are likely initiated by the heterogeneous dissociation of  $\text{Cl}_2$  on the wall [1,2]. The thermal chlorination of  $\text{CHCl}_3$  in flow systems [3–7] is one example amongst others.

This work aims to present new experimental results for this reaction. They have been obtained in a conditioned static system and show a typical increase of the reaction rate with time that is not reported in previous works [1,3–7]. This auto-acceleration can be quantitatively explained by the decomposition of the

$\text{CCl}_4$  produced. The reaction model used is an entirely homogeneous radical mechanism and its known associated kinetic and thermodynamic parameters. It involves the reaction couple  $\text{CHCl}_3 + \text{Cl} = \text{CCl}_3\cdot + \text{HCl}$  and the thermal reactions of  $\text{CCl}_4$ . These latter have recently been modeled [8] and the values of their parameters are thus checked in this work.

## EXPERIMENT AND MODELING

$\text{CHCl}_3$  (Merck) was purified by preparative gas chromatography and contained less than 0.005% impurity.  $\text{Cl}_2$  (Matheson, ultra-high purity), 99.9% pure, was used without further purification. Both reagents were degassed at  $-196^\circ\text{C}$  on the vacuum line at pressures below  $10^{-5}$  Torr before their introduction into the reaction cell. The conventional static system, procedure, and photometric and gas chromatographic analyses

Correspondence to: G. Huybrechts (ghuybrec@vub.ac.be)

\* Present address: Exxon Chemical Polymers International, Canadastraat 20, B-2070 Zwijndrecht, Belgium

© 2000 John Wiley & Sons, Inc.

were similar to those in [9,10]. Reactions were carried out in two cylindrical quartz reaction vessels unpacked (100 ml) and packed (70 ml) with quartz tubing with surface-to-volume ratios,  $S/V$ , of about 1.4 and  $10 \text{ cm}^{-1}$ , respectively. The reactor walls were conditioned by pyrolyzing pure  $\text{CHCl}_3$  at high temperature (729 K) until reproducible kinetic results were obtained in the absence as well as in the presence of  $\text{Cl}_2$ . The kinetics of the reaction were followed by continuously monitoring the absorption of  $\text{Cl}_2$  at 350 nm in the unpacked reaction cell. Introduction of amounts of  $\text{CHCl}_3$ ,  $\text{CCl}_4$ , and  $\text{HCl}$  into the cell showed that

these compounds do not absorb at this wavelength and thus do not affect the  $\text{Cl}_2$  measurement. Due to the presence of quartz tubes, the experiments performed in the packed reactor had to be carried out without photometric monitoring of the  $\text{Cl}_2$  pressure. The variation of the total pressure was measured with a Pyrex Bourdon gauge, capable of detecting pressure changes of 0.1 Torr. The gas chromatographic analyses (katharometer detector) were carried out on a 3-m column containing 30% by weight of Silicone SE 30 on 60–80 mesh Chromosorb PAW. After 14 min, the temperature of the column was raised from 80 to  $140^\circ\text{C}$

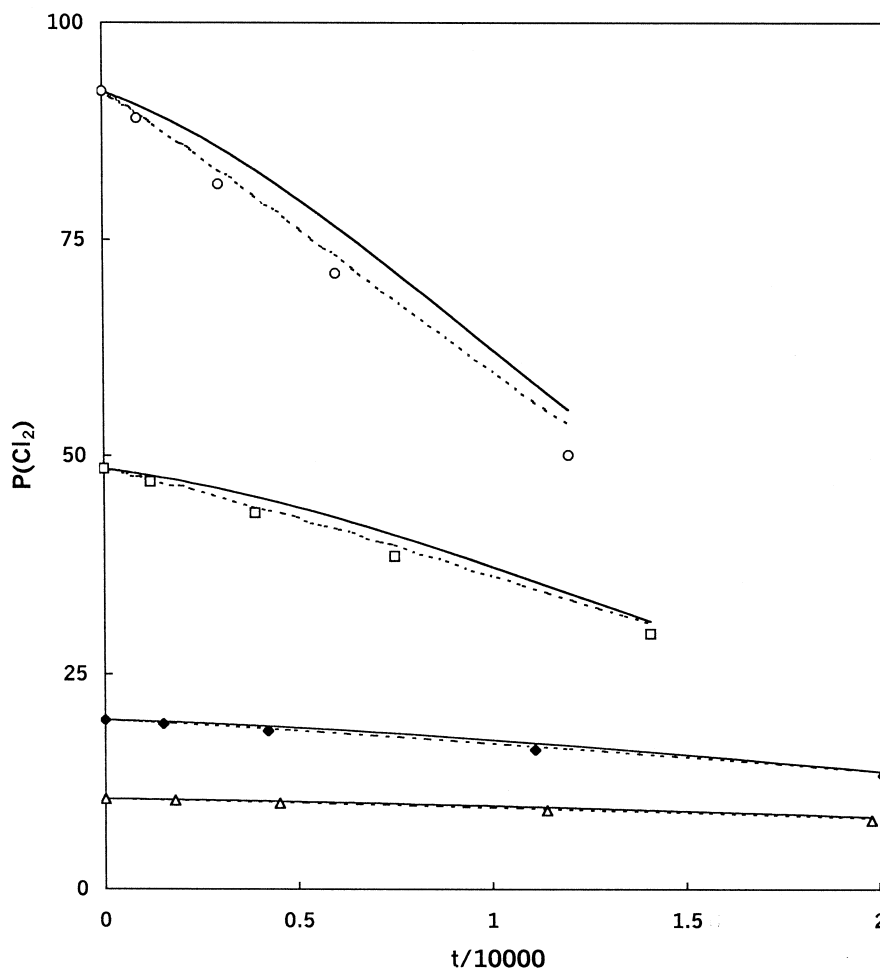


**Figure 1** Pressure of  $\text{Cl}_2$  ( $p(\text{Cl}_2)$  in Torr) vs. reaction time ( $t$  in s) at 573 K for varying initial pressures of  $\text{Cl}_2$ .

- $\triangle$ :  $p(\text{Cl}_2)_0 = 10.5$  and  $p(\text{CHCl}_3)_0 = 90.4$  Torr
- $\blacklozenge$ :  $p(\text{Cl}_2)_0 = 19.7$  and  $p(\text{CHCl}_3)_0 = 92.1$  Torr
- $\square$ :  $p(\text{Cl}_2)_0 = 48.5$  and  $p(\text{CHCl}_3)_0 = 91.7$  Torr
- $\circ$ :  $p(\text{Cl}_2)_0 = 92.1$  and  $p(\text{CHCl}_3)_0 = 93.0$  Torr

Full curves: simulations with the reaction model given in Tables I and II wherein only parameters involving  $\text{CHCl}_3$  are slightly adjusted. Dotted curves: simulations with a model wherein some parameters of the thermal reactions of  $\text{CCl}_4$  are slightly adjusted, too (see text)

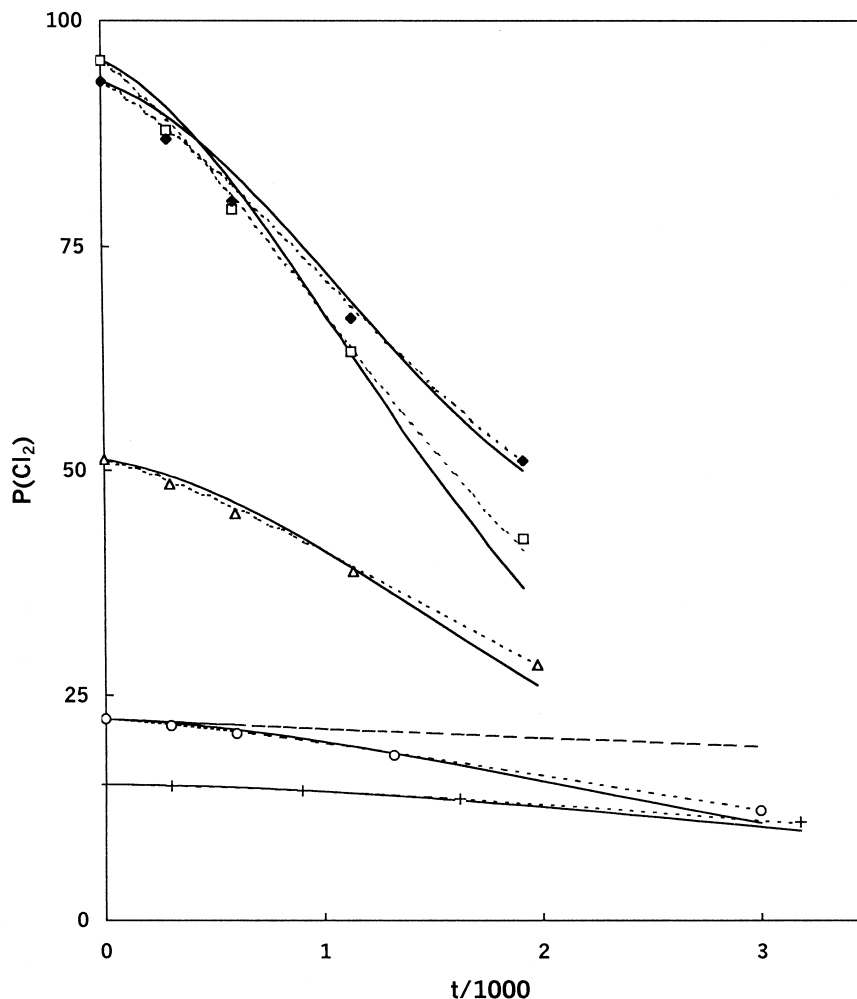


**Figure 2** Pressure of  $\text{Cl}_2$  ( $p(\text{Cl}_2)$  in Torr) vs. reaction time ( $t$  in s) at 615 K for varying initial pressures of  $\text{Cl}_2$  and  $\text{CHCl}_3$ .

- + :  $p(\text{Cl}_2)_0 = 15.2$  and  $p(\text{CHCl}_3)_0 = 14.0$  Torr
- O :  $p(\text{Cl}_2)_0 = 22.4$  and  $p(\text{CHCl}_3)_0 = 92.0$  Torr
- Δ :  $p(\text{Cl}_2)_0 = 51.2$  and  $p(\text{CHCl}_3)_0 = 96.4$  Torr
- ◆ :  $p(\text{Cl}_2)_0 = 93.3$  and  $p(\text{CHCl}_3)_0 = 49.2$  Torr
- :  $p(\text{Cl}_2)_0 = 95.7$  and  $p(\text{CHCl}_3)_0 = 95.4$  Torr

Full curves: simulations with the reaction model given in Tables I and II wherein only parameters involving  $\text{CHCl}_3$  are slightly adjusted. Dotted curves: simulations with a model wherein some parameters of the thermal reactions of  $\text{CCl}_4$  are slightly adjusted, too (see text). Dashed curve: simulation with the reaction model given in Tables I and II wherein the Step -4 has been suppressed.

at 20°C/min.  $\text{H}_2$  was used as a carrier gas with a flow of 3 L/h. The simulated and optimized  $\text{Cl}_2$ -pressure-time curves were obtained using OPTKIN, a user-friendly PC program for mechanistic modeling of reactions by kinetic and thermodynamic parameter optimization [11]. Applications of this program and examples of the modeling strategy are to be found in [8,10,12,13]. The sensitivity analyses were also performed with OPTKIN.

## EXPERIMENTAL RESULTS

The thermal chlorination of  $\text{CHCl}_3$  has been studied between 573 and 635 K with initial pressures ranging from 10.5 to 95.7 Torr for  $\text{Cl}_2$  and 14.0 to 97.2 Torr for  $\text{CHCl}_3$ . The total pressure was varied between 29.2 and 191.1 Torr. No inert gases were used. As shown by the photometric and gas chromatographic analyses, the reaction stoichiometry is



up to conversions close to 100%. No pressure change is observed (within the detection limits) in agreement with equation (A). In some experiments, trace amounts of  $\text{C}_2\text{Cl}_6$  (less than 0.01%) are formed. No other products are detected.

The kinetics of the reaction were studied by following the consumption of  $\text{Cl}_2$ . The chlorination in the clean-walled reaction vessel is very fast and strongly heterogeneous. All the results reported hereafter refer to reproducible slower reactions in totally conditioned reaction cells.

Experimental  $\text{Cl}_2$  profiles for a series of experiments carried out in the unpacked cell are represented in Figures 1 ( $T = 573 \text{ K}$ ), 2 ( $T = 615 \text{ K}$ ), and 3 ( $T = 635 \text{ K}$ ). As can be seen from Figures 2 and 3, these profiles show an S-shape at the higher temperatures. The first part of the S-shape corresponds to an auto-acceleration. This auto-acceleration seems to be negligible at the lower temperature (see Fig.1). Notice, however, that the chlorine consumption rate depends on the initial chlorine pressure (the initial  $\text{CHCl}_3$  pressure is almost constant) but that it remains almost constant in the course of time while the chlorine pressure decreases. All these findings are too complicated to be

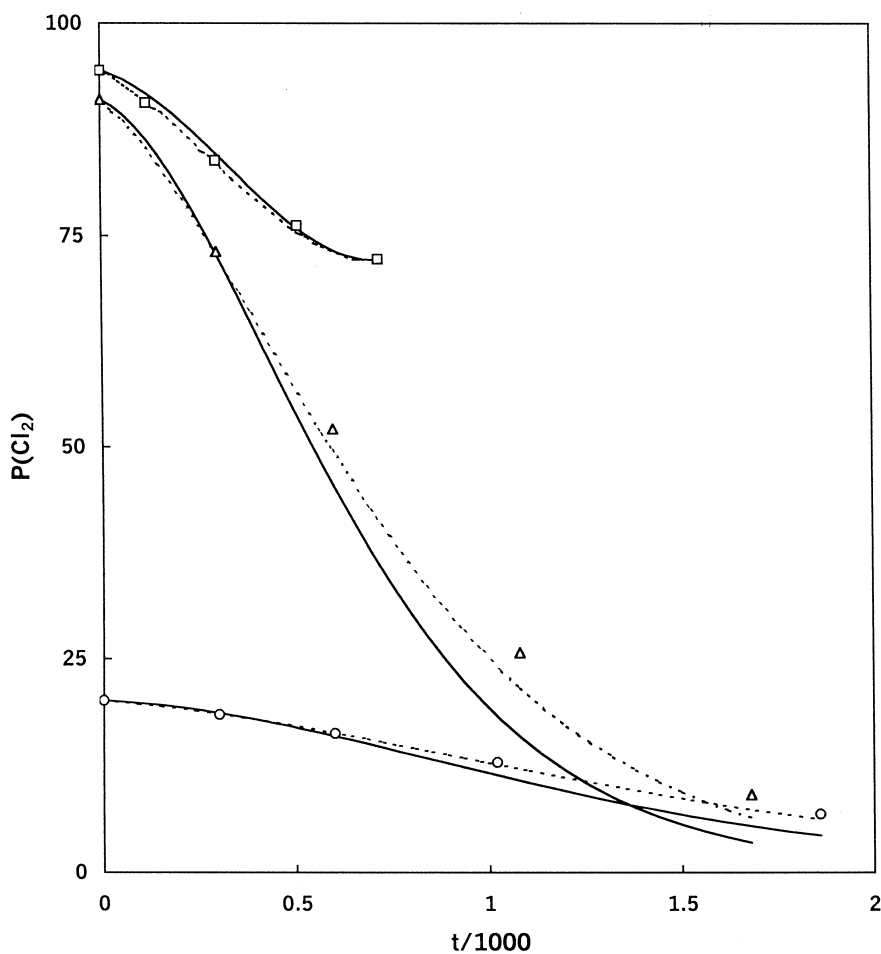


**Figure 3** Pressure of  $\text{Cl}_2$  ( $p(\text{Cl}_2)$  in Torr) vs. reaction time ( $t$  in s) at 635 K for varying initial pressures of  $\text{Cl}_2$  and  $\text{CHCl}_3$ .

- :  $p(\text{Cl}_2)_0 = 20.1$  and  $p(\text{CHCl}_3)_0 = 97.2$  Torr
- △:  $p(\text{Cl}_2)_0 = 91.0$  and  $p(\text{CHCl}_3)_0 = 91.3$  Torr
- :  $p(\text{Cl}_2)_0 = 94.4$  and  $p(\text{CHCl}_3)_0 = 22.3$  Torr

Full curves: simulations with the reaction model given in Tables I and II wherein only parameters involving  $\text{CHCl}_3$  are slightly adjusted. Dotted curves: simulations with a model wherein some parameters of the thermal reactions of  $\text{CCl}_4$  are slightly adjusted, too (see text).

simply described by a classical empirical rate equation. The experimental results will therefore be presented in terms of  $\text{Cl}_2$  profiles obtained by a combined numerical modeling-optimization procedure.

Note finally that a slight heterogeneous effect is detected by carrying out experiments in the packed reactor with a 7-fold increase in the surface-to-volume ratio. As shown by GC-analyses, the formation of  $\text{CCl}_4$  proceeds about 40% faster than in the unpacked reaction cell for a typical experiment ( $T = 615 \text{ K}$ ,  $p(\text{CHCl}_3)_o = 93.0 \text{ Torr}$ ,  $p(\text{Cl}_2)_o = 92.1 \text{ Torr}$ ).

## NUMERICAL MODELING AND DISCUSSION OF THE RESULTS

All the experimental results can be quantitatively explained by the reaction model presented in Tables I and II. It was obtained using a combined simulation-optimization-reduction procedure from OPTKIN, starting from a larger model comprising all the known steps of the pyrolyses of  $\text{CCl}_4$  and  $\text{C}_2\text{Cl}_6$  [8] together with Steps 2 and -2. Indeed, for the homogeneous

thermal chlorination of  $\text{CHCl}_3$  to  $\text{CCl}_4$  under the experimental conditions of this work,  $\text{CCl}_4$  is not stable. With Steps 2 and -2 as the starting point, all additional reaction steps involved in the model from [8] are expected to be important. Elementary reactions that could be eliminated are those involving  $\text{C}_2\text{Cl}_6$  (and its issuing  $\text{C}_2\text{Cl}_5$  radical), which is produced only in trace amounts in the thermal chlorination of  $\text{CHCl}_3$ . All experimental data from Figures 1 to 3 were involved as one set in the reduction procedure.

The homogeneous radical mechanism and its kinetic parameters are given in Table I. Sensitivity analyses as a function of reaction time show that all reactions play a significant role. Note that the back reactions -1, -2, -3, and -5 are only of importance for those experiments where the simulation is carried out up to high consumption of  $\text{CHCl}_3$  or  $\text{Cl}_2$ . The thermodynamic parameters are given in Table II. Almost all these kinetic and thermodynamic parameters are from [8] and are optimized parameters that fit the experimental kinetic results on the thermal reactions of  $\text{CCl}_4$  and  $\text{C}_2\text{Cl}_6$ . Only those for reaction 2 and compound  $\text{CHCl}_3$  were slightly adjusted by optimization

**Table I** Kinetic Model for the Thermal Chlorination of  $\text{CHCl}_3$

Homogeneous Elementary Reaction Steps	$E$	$\log_{10}A$	Rem.
<i>Primary:</i>			
Initiation: $\text{Cl}_2 + \text{M} \xrightarrow{1} 2\text{Cl} + \text{M}$	55.85	12.94	a,b
Propagation: $\text{Cl} + \text{CHCl}_3 \xrightarrow{2} \text{HCl} + \text{CCl}_3\cdot$	3.65	9.73	c
$\text{CCl}_3\cdot + \text{Cl}_2 \xrightarrow{3} \text{CCl}_4 + \text{Cl}$	5.10	8.70	d
Transfer: $\text{CCl}_3\cdot + \text{HCl} \xrightarrow{-2} \text{Cl} + \text{CHCl}_3$	11.79	8.38	a
$\text{CCl}_4 + \text{Cl} \xrightarrow{-3} \text{CCl}_3\cdot + \text{Cl}_2$	15.66	10.82	a
Termination: $2\text{Cl} + \text{M} \xrightarrow{-1} \text{Cl}_2 + \text{M}$	-1.63	9.11	e
$\text{CCl}_3\cdot + \text{Cl} \xrightarrow{4} \text{CCl}_4$	0.00	10.86	d
$\text{CCl}_3\cdot + \text{CCl}_3\cdot \xrightarrow{5} \text{C}_2\text{Cl}_6$	0.00	9.67	d
<i>Secondary:</i>			
Decomposition: $\text{CCl}_4 \xrightarrow{-4} \text{CCl}_3\cdot + \text{Cl}$	68.04	16.82	a
$\text{C}_2\text{Cl}_6 \xrightarrow{-5} \text{CCl}_3\cdot + \text{CCl}_3\cdot$	67.09	17.40	a

The activation energies  $E$  are expressed in kcal/mol and the A factors in L, mole, s-units.

<sup>a</sup> Calculated using the principle of microreversibility in the computer program from the thermodynamic data given in Table II and the rate constant of the corresponding back reaction at the mean temperature of all experiments.

<sup>b</sup> Due to the lack of experimental data for the third body efficiencies, it is assumed that the rate constant of the back reaction is the same for  $\text{M} = \text{CHCl}_3$ ,  $\text{HCl}$ , and  $\text{CCl}_4$  and equal to that for  $\text{M} = \text{Cl}_2$ . Simulations using different values for third body collision efficiencies show little effect.

<sup>c</sup> The values of the Arrhenius parameters are values optimized in this work. The initial values used in the optimization procedure ( $E = 3.35 \text{ kcal/mol}$  and  $\log_{10}A = 9.84$ ) are from [14,15].

<sup>d</sup> Optimized value from [8].

<sup>e</sup> From [16,17], not optimized in [8].

**Table II** Heats of Formation  $\Delta H_f^\circ$  (kcal/mol), heat capacities  $C_{p,T}^\circ = a + bT + cT^2$ , and entropies  $S^\circ$  (Gibbs/mol) based on a 1-atm standard state

Compound	$\Delta H_{f,298}^\circ$	$S_{298}^\circ$	$C_{p,T}^\circ$			Rem.
			a	$10^2 \cdot b$	$10^5 \cdot c$	
Cl <sub>2</sub>	0.0	53.3	7.07	0.426	-0.25	a
HCl	-22.1	44.7	7.19	-0.114	0.161	b
CHCl <sub>3</sub>	-24.7	70.8	7.49	3.12	-1.73	c
CCl <sub>4</sub>	-22.2	73.8	12.8	3.00	-1.93	a
C <sub>2</sub> Cl <sub>6</sub>	-33.2	95.2	19.9	5.35	-3.32	a
Cl	29.0	39.5	4.72	0.225	-0.179	a
CCl <sub>3</sub> ·	18.0	71.2	9.87	2.24	-1.41	a

<sup>a</sup> From [13].

<sup>b</sup> From [18].

<sup>c</sup> The values of  $\Delta H_{f,298}^\circ$  and  $S_{298}^\circ$  are values optimized in this work. The initial values (-24.6 and 70.6, respectively) used in the optimization procedure are from [19].

in this work (see legends of Tables I and II, respectively).

The fitting of the experimental Cl<sub>2</sub> profiles is represented by the curves in Figures 1–3 and is quite satisfactory. Note that the simulation of the experimental results without any adjustments of the kinetic and thermodynamic parameters is scarcely poorer (the profiles are never lower by more than 10%). As can also be seen in Figures 1–3, the fitting is much better if some parameters of the thermal reactions of CCl<sub>4</sub> are also slightly modified by optimization (corrections do not exceed  $\pm 0.3$  kcal/mol for activation energies and heats of formation,  $\pm 0.3$  log units for A factors, and 0.5 Gibbs/mol for entropies). This illustrates the reliability of the parameters optimized in [8] between 651 and 718 K and used in this study at lower temperatures ranging from 573 to 635 K.

A series of simulations have been performed using

the kinetic model, for example for the experiment of Figure 2 with  $p(\text{Cl}_2)_0 = 22.4$  Torr. As can be seen in Figure 4, the secondary source of Cl atoms (Step -4) is already as fast as the primary source (Step 1) after only about 150 s (0.8% reaction). After 3000 s (50% Cl<sub>2</sub> consumption), it is even more than 100 times faster. The decomposition in Step -4 of the CCl<sub>4</sub> produced by the chain propagation Step 3 is therefore the origin of the observed auto-acceleration. This is confirmed in Figure 2, which shows that the auto-acceleration disappears when Step -4 is not taken into account. This occurs for all experiments. It should be pointed out here that the study of the kinetics of the gas-phase photochlorination of CHCl<sub>3</sub> [20] is not affected by the decomposition of CCl<sub>4</sub> owing to the lower temperatures used (303–426 K). The simulations also show that the recombination of the CCl<sub>3</sub>

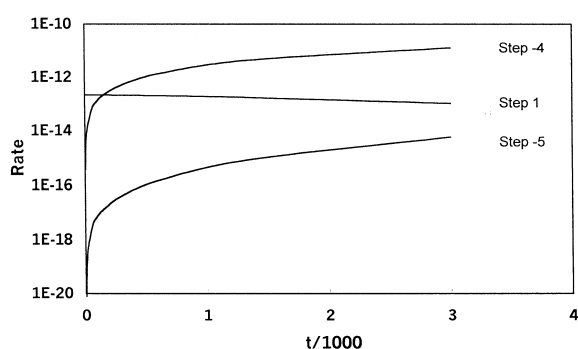


**Figure 4** Rates (in mol/L · s) of initiation steps vs. reaction time ( $t$  in s) at 615 K. Initial pressures of Cl<sub>2</sub> and CHCl<sub>3</sub> of 22.4 and 92.0 Torr, respectively. Simulations with the reaction model given in Tables I and II.

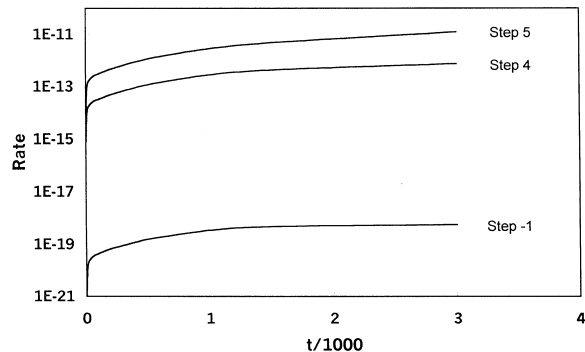


**Figure 5** Rates (in mol/L · s) of termination steps vs. reaction time ( $t$  in s) at 615 K. Initial pressures of Cl<sub>2</sub> and CHCl<sub>3</sub> of 22.4 and 92.0 Torr, respectively. Simulations with the reaction model given in Tables I and II.

radicals (Step 5) is the fastest chain termination (see Fig. 5) and that this step has produced about 0.005%  $C_2Cl_6$  at the end of the experiment. The calculated initial chain length (rate of Step 3/rate of Step 5) is as high as  $10^5$ . The simulations show finally that a surface controlled removal of Cl atoms would play a role if its efficiency  $\varepsilon(Cl)^*$  is not lower than about  $3 \times 10^{-5}$ . The lowest limit value of  $\varepsilon(Cl)$  measured for "poisoned" walls is ca.  $10^{-5}$  [21,22]. It therefore seems likely that the experiments were carried out in a well-conditioned reaction vessel.

Taylor and Hanson [3] and Aver'yanov et al. [5] suggested that the heterogeneous wall-initiated dissociation of  $Cl_2$  may occur much faster than the homogeneous initiation step 1 (see Table I). Nevertheless, Taylor and Hanson [3] observed an increase of only 10% of the overall chlorination rate for a seven-fold increase of the surface-to-volume ratio of the reactor (similar to our observations). If, however, the chain termination should occur also entirely heterogeneously on the wall of the reaction cell, a heterogeneous increase of the rate constant of the reaction 1 in the packed cell might be obscured by a greater chain termination efficiency. The overall reaction rates reported in [3] and [5] are, however, at least 10 times higher than observed in this work. This may suggest a difference in the conditioning of the reaction cell or an effect of impurities. Indeed, we observed that when a reaction cell has been exposed to  $O_2$ , the next runs proceeded much faster. The conditioning of the reaction cell then had to be renewed. Note that simulations show that the reaction rates observed in [1,3-7] require a chain initiation step of the type  $Cl_2 \rightarrow 2Cl$ , which would be at least  $10^4$  times faster than the homogeneous step 1 and are therefore most probably catalyzed by the wall.

In conclusion, the thermal chlorination of  $CHCl_3$  studied in this work can be simulated with a kinetic model that is entirely homogeneous. This model is an additional check of the validity of a good model for the pyrolyses of  $CCl_4$  [8] and  $C_2Cl_6$  [8,10] between 651 and 718 K. Indeed, almost all of its reaction steps and parameters are the same and were used at lower temperatures ranging from 573 to 635 K.

\*  $\varepsilon(Cl)$  = rate of removal of Cl atoms per unit surface/rate of collision of Cl atoms per unit surface given by kinetic theory of gases.

Y. Hubin wishes to thank IWONL for a grant.

## BIBLIOGRAPHY

1. Ashmore, P. G.; Spencer, M. S. *Trans Faraday Soc* 1964, 60, 1608.
2. Amorebieta, V. T.; Colussi, A. J. *Int J Chem Kinet* 1985, 17, 849.
3. Taylor, A.; Hanson, W. E. *J Chem Phys* 1939, 7, 418.
4. Arai, T.; Ioshida, M.; Shinoda, K. *J Chem Soc Japan* 1958, 61, 1231.
5. Aver'yanov, V. A.; Lebedev, N. N.; Lebedeva, G. F. *Russ J Phys Chem* 1977, 51, 1652.
6. Aver'yanov, V. A.; Lebedev, N. N.; Lebedeva, G. F. *Kinet Katal* 1979, 20, 78.
7. Rozlovskii, A. I. *Kinet Katal* 1982, 23, 734.
8. Huybrechts, G.; Narmon, M.; Van Mele, B. *Int J Chem Kinet* 1996, 28, 27.
9. Huybrechts, G.; Hubin, Y. *Int J Chem Kinet* 1986, 18, 497.
10. Huybrechts, G.; Theys, J.; Van Mele, B. *Int J Chem Kinet* 1996, 28, 755.
11. Huybrechts, G.; Van Assche, G. *Comput Chem* 1998, 22, 413.
12. Huybrechts, G.; Hubin, Y.; Van Mele, B. *Int J Chem Kinet* 1989, 21, 575.
13. Huybrechts, G.; Van Assche, G.; Van der Auwera, S. *Int J Chem Kinet* 1998, 30, 359.
14. Knox, J. H. *Trans Faraday Soc* 1962, 58, 275.
15. NIST Chemical Kinetics Database, version 6.0, Standard Reference Data Program, U.S. Department of Commerce, NIST 1994.
16. Baulch, D. L.; Duxbury, J.; Grant, S. J.; Montague, D. C. *J Chem Rev Data* 1981, 10, Supplement 1.
17. Westley, F.; Fizzell, D. H.; Herron, J. T.; Hampson, R. F.; Mallard, W. G. NIST Chemical Kinetics Database, 1998.
18. Stull, D. R.; Westrum, E. F.; Sinke, G. C. *The Chemical Thermodynamics of Organic Compounds*; Wiley: New York, 1969.
19. Rodgers, A. S.; Chao, J.; Wilhoit, R. C.; Zwolinski, B. *J. J Phys Chem Ref Data* 1974, 3, 117.
20. De Maré, G. R.; Huybrechts, G. *Trans Faraday Soc* 1968, 64, 1311.
21. Ashmore, P. G.; Parker, A. J.; Stearne, D. E. *Trans Faraday Soc* 1971, 67, 3081.
22. Ashmore, P. G.; Gardner, J. W.; Owen, A. J.; Smith, B.; Sutton, P. R. *J Chem Soc, Faraday Trans 1*, 1982, 78, 657.